Journal of Pain Research

Dovepress
open access to scientific and medical research

Open Access Full Text Article

ORIGINAL RESEARCH

Fecal Microbiota Transplantation Alleviated Paclitaxel-Induced Peripheral Neuropathy by Interfering with Astrocytes and TLR4/p38MAPK Pathway in Rats

Haibin Shi[1], Minmin Chen[2], Caihong Zheng[2], Bian Yinglin[2], Bin Zhu[2]

[1]Department of Anesthesiology, the Affiliated Hangzhou First People's Hospital, Zhejiang University School of Medicine, Hangzhou, Zhejiang, People's Republic of China; [2]Department of Anesthesiology, Hangzhou Women's Hospital, Hangzhou, Zhejiang, People's Republic of China

Correspondence: Bin Zhu, Department of Anesthesiology, Hangzhou Women's Hospital, 369 Kunpeng, Shangcheng District, Hangzhou City, Zhejiang Province, 310000, People's Republic of China, Tel +86 13758136317, Email zhubinhfy@163.com

Purpose: Paclitaxel-induced peripheral neuropathy (PIPN) constitutes a refractory and progressive adverse consequence of paclitaxel treatment, causing pain and sensory anomalies in cancer survivors. Although the gut-brain axis is involved in multiple disorders including cancer, its impact on peripheral pain conditions remains elusive. Thus, we assessed the importance of gut microbiota and related mechanisms in PIPN.

Methods: By implementing fecal microbiota transplantation (FMT) in a rat PIPN model (ie, rats treated with paclitaxel; hereafter as PIPN rats), we explored the effect of gut microbiota on PIPN rats using multiple methods, including different behavioral tests, 16S ribosomal DNA (rDNA) sequencing, and biochemical techniques.

Results: Sequencing of 16S rDNA revealed that the abundance of genera *Bacteroides* and *UCG-005* increased, while that of genera *Turicibacter, Clostridium sensu stricto 1* and *Corynebacterium* decreased in the PIPN rats. However, when treated with FMT using fecal from normal rats, the mechanical allodynia and thermal hyperalgesia in PIPN rats were significantly alleviated. In addition, FMT treatment reduced the expression of toll-like receptor 4 (TLR4), phospho-p38 mitogen-activated protein kinase (p-p38MAPK), and the astrocytic marker glial fibrillary acidic protein in the colon and spinal dorsal horn. TAK242 (a TLR4 inhibitor) significantly alleviated the behavioral hypersensitivity of PIPN rats and inhibited the TLR4/p38MAPK pathway in astrocytes in these rats.

Conclusion: The gut microbiota played a critical role in PIPN. Future therapies treating PIPN should consider microbe-based treatment as an option.

Keywords: astrocyte, gut microbiota, paclitaxel, p38, peripheral neuropathy, TLR4

Introduction

Chemotherapeutic drugs, such as paclitaxel, are widely used in treating patients with tumors,[1] such as breast cancer,[2,3] ovarian cancer,[4,5] and lung cancer.[6] However, these drugs can cause adverse consequences, including chemotherapy-induced peripheral neuropathy (specifically, for paclitaxel, it is known as paclitaxel-induced peripheral neuropathy (PIPN)). PIPN occurs in about 97% of patients receiving paclitaxel treatment, significantly affecting these patients' quality of life.[7] The main symptoms include pain, numbness, paresthesia and hypersensitivity to mechanical or cold stimuli.[8] The underlying mechanisms regulating PIPN remain elusive, but inflammatory cytokines are presumably involved in the pathogeny of this adverse event.[9] Nowadays, PIPN remains a challenge for patients receiving chemotherapy.

Toll-like receptor 4 (TLR4) regulates pain chronification.[10,11] The activity of TLR4 combined with mitogen-activated protein kinases (MAPKs) has been previously documented in PIPN.[12] During the initiation and progression of PIPN, TLR4 was activated in the astrocytes of the spinal cord.[13] This activation further triggers the release of interleukin-1β (IL-1β) and tumor necrosis factor-alpha (TNF-α), among others, which can sensitize nociceptive neurons and trigger

Received: 25 April 2023
Accepted: 9 July 2023
Published: 17 July 2023

neurogenic inflammation.[14] Similarly, the activation of astrocytes can contribute to neuroinflammation and central sensitization in PIPN.[15–17] Thus, the pathophysiology of PIPN likely involves astrocytes, TLR4, and downstream MAPKs.

Gut microbiota represents the diversified microorganisms residing within an individual's gastrointestinal tract.[18,19] The gut-brain axis defines a bidirectional cross-talk between the gut bacterial community and brain through a network of signaling systems involved in host physiology,[20] metabolism[21,22] and neurodegenerative disorders.[23,24] An interruption in the balance of the microbiota can lead to dysbiosis, affecting the onset and progression of several pathologies, eg, inflammatory bowel disease,[25] irritable bowel syndrome,[26] neuropsychiatric disorders,[27,28] and other pain conditions.[29,30] A large number of PIPN events linked with gut microbiota dysbiosis were observed in recent years.[31,32] For instance, in Parkinson's disease, fecal microbiota transplantation (FTM) reduced dysbiosis and astrocytes activation in the brain.[33,34] However, currently, no clear evidence indicates an essential function of gut microbiota, astrocytes, and the TLR4 pathway in PIPN. Thus, we performed multiple experiments aimed at investigating the gut microbiota and corresponding regulating mechanisms in rat PIPN.

Materials and Methods

Experimental Rats

Adult male Sprague-Dawley rats, purchased from Slack Laboratory Animal Co. (Shanghai, China), were randomly housed in ventilated cages (maximum 3 in each cage) under a 12/12 light-dark cycle, with standard food and water. Temperature was controlled at 22 ± 1°C, while humidity was set at 65–75%. Before being used for experiments, acclimatization to the surrounding environment was allowed for five days. The study was conducted in accordance with the National Institutes of Health Guidelines for the Care and Use of Laboratory Animals and was approved by the Institutional Animal Care and Use Ethical Committee of Zhejiang Chinese Medical University (batch number 20191028–06). During the study, investigators were blinded to experimental administrations.

Paclitaxel-Induced Peripheral Neuropathy (PIPN) Rat Model

Paclitaxel (Bristol-Myers Squibb, Princeton, NJ) was diluted with 0.9% saline and administered intraperitoneally every other day (2 $mg \cdot kg^{-1}$ each time for 4 injections in total) to establish the PIPN model, as described in previous reports.[11,35,36] Rats in the Vehicle group were similarly injected with an equal volume of the Vehicle containing a polyoxyethylene castor oil derivative (Cremophor EL) and ethanol diluted in 0.9% saline. Rats were carefully observed for any abnormal spontaneous behaviors during treatment.

Antibiotic Treatment

Based on previous reports,[37,38] rats were given broad-spectrum antibiotics (Abx), ie, a mixture of vancomycin (0.5 $g \cdot L^{-1}$), ampicillin (1.0 $g \cdot L^{-1}$), metronidazole (1.0 $g \cdot L^{-1}$), and neomycin (1.0 $g \cdot L^{-1}$). Antibiotics with sucralose (3 $g \cdot L^{-1}$) were administered starting seven days before paclitaxel administration and continued throughout the experimental period. When necessary, oral antibiotics were administered by gastric gavage. All antibiotics were provided by Solarbio Science and Technology Co., Ltd. (Beijing, China).

Fecal Microbiota Transplantation (FMT) Treatment

Fresh fecal samples were collected from rats in the Vehicle using sterile tubes. The samples were immediately frozen in liquid nitrogen and stored at −80°C. After pooling the samples, a total of 10 g feces were diluted, soaked, and shaken in 10 mL sterile phosphate-buffered saline solution (ie, 10 g fecal pellets/10 mL PBS) for ~15 minutes (min), and spun at 1000 rpm at 4°C for 5 min. Then, supernatant was collected and further spun at 8000 rpm at 4°C for 5 min. The pellet (ie, bacteria collected from the feces) was then resuspended in PBS and filtered twice, and then deposited at −80°C until transplantation. When used, recipient rats were orally administered the prepared bacteria suspension (2 mL) daily for 23 days.

Intrathecal Injection of Drugs

Intrathecal injections were performed following a previous description.[35] In brief, the experimental animals were lightly anesthetized and a 25-gauge needle (attached to a 25-μL Hamilton syringe) was inserted in the L4-L5 intervertebral space. An observed tail-flick response indicated that the intrathecal injection succeeded. The needle stayed in place for more than 15 seconds (s) to ensure drug delivery. One day before establishing the rat PIPN model, either astrocytic inhibitor fluorocitrate (10 nmol/10 μL, Sigma-Aldrich, United States), lipopolysaccharide (LPS) (20 μg/10 μL, Beyotime Biotechnology Co., Ltd., China), TLR4 inhibitor TAK242 (20 μg/10 μL, Sigma-Aldrich, United States), p38 inhibitor SB203580 (20 μg/10 μL, Sigma-Aldrich, United States), or sterile saline (10 μL) were injected intrathecally. Drug doses were used based on previous reports.[12,39–41]

Behavioral Tests

Mechanical Withdrawal Threshold Measurements (MWTs)

Mechanical withdrawal threshold measurements (MWTs) were measured with the SLY-HFM hand-held dynamometer (Beijing Shuolinyuan Technology Co., Ltd., China). When measuring, each rat was positioned in a transparent chamber with a wire mesh floor and allowed to acclimate to the surrounding environment for at least half an hour. The hand-held dynamometer measuring pressure pain thresholds was used to simulate the rat for 1–2 s with an interval of 30s. The stimulation procedure was repeated 5 times. The average value was defined as MWT. The pain measuring device automatically recorded the pressure value related to the mechanical stimulus in grams. Rapid paw withdrawal, flinching, or licking were considered positive responses.

Thermal Withdrawal Latency Measurements (TWLs)

Thermal withdrawal latency measurements (TWLs) were assessed by radiant heat stimulation (Chengdu Tai Meng Software Co., Ltd., China). Rats were put in transparent chambers with a glass floor and acclimated to the environment for at least half an hour. Then, we applied a radiant thermal stimulus to the hind paw at the plantar surface from beneath the floor. The interval between light onset and paw lift was recorded and defined as TWL. Stimulation was repeated five times with at least 5 min of rest. Due to considerable variability in the first two measurements, the average TWL of the last three measurements was used as a threshold for thermal-evoked pain.

Western Blotting

Rats were sacrificed under deep anesthesia; the colon tissues were promptly harvested and subjected to protein extraction using RIPA buffer and lysed. After centrifuging at 1500 relative centrifugal force (RCF) (15 min at 4°C). The concentration was determined using the BCA kit (Beyotime, China), and the rest of supernatant was stored at −80°C. Proteins were separated via 10% SDS-PAGE (Genshare Biology, China) and transferred to PVDF membranes (Millipore, Burlington, MA, United States), which were blocked in 5% non-fat milk, and incubated at 4°C overnight with either rabbit anti-TLR4 (1:1000, CST), rabbit anti-p38 (1:1000, CST), rabbit anti-pro-p38 (1:1000, CST), or mouse anti-GAPDH (1:1000, Zhongshan Golden Bridge Biotechnology) primary antibodies. The next day, the membranes were incubated with the secondary antibodies (ie, horseradish peroxidase-conjugated anti-mouse or rabbit secondary antibodies (1:5000 for both, Jackson ImmunoResearch, USA)). The visualization was via the Clarity Western ECL Substrate (EMD Millipore) and the quantification of band intensities was via the Fiji ImageJ software.

Immunohistochemistry

The anesthetized rats were transcranially perfused with PBS and 4% neutral buffered paraformaldehyde. Subsequently, the colon and spinal cord (L3-L5 region) tissues were excised, immersed in 4% neutral buffered paraformaldehyde and dewatered in sucrose solution (30%, diluted in water) at 4°C for two days.[42] After embedding, tissues were sectioned serially (thickness: 5 μm) using cryostat (Leica, SQ2125). The slices were then deparaffinized, incubated with 3% H_2O_2 (10 min), washed with PBS (3 times for 3 min each), and incubated with 5% bovine serum albumin (BSA) at 25°C for half an hour.[43] Primary antibodies targeting GFAP (1:100, CST) were applied to stain the sections, which were incubated at 25°C for one hour. After washing the slices with PBS 3 times for 3 min each, they were incubated with the secondary antibody (polymerized horseradish peroxidase-conjugated goat anti-rabbit IgG (Boster Company, Wuhan, China) for half an hour at 25°C and subsequently washed again with PBS 3 times

for 3 min each. All slides were exposed to DAB (Vector Labs) and counterstained with hematoxylin. Fluorescence intensity scoring was utilized to assess reactivity by determining the percentage of positively stained cells in images at 200× magnification captured from the left and right dorsal horn regions. The values obtained for the left and right dorsal horn were averaged for each spinal cord slice, and three slices were randomly analyzed for each group.

16S rDNA Sequencing

Upon completing the experiments, defecated stools were gathered from each group. The fecal microbial analysis was conducted utilizing the 16S rDNA sequencing method. Specifically, the extracted genomic DNA was amplified by PCR, with the amplified products being quantified utilizing the QuantiFluor-ST quantification system (Promega, United States). MiSeq library was prepared and sequenced through the TruSeq DNA Sample Prep Kit (Illumina, USA). The raw reads were quality-controlled using Trimmomatic software package. Amplicon sequence variants (ASVs) were obtained and community composition and species differences were analyzed. The α-diversity analysis was examined to measure the microbial diversity indices. The β-diversity analysis was examined to measure how different samples varied in terms of species complexity.

Enzyme-Linked Immunosorbent Assay

Rat IL-1β and TNF-α ELISA kits were obtained from Solarbio Science and Technology Co., Ltd. (Beijing, China). All experimental protocols adhered to the manufacturer's instructions.

Experimental Groups and Treatments

As shown in Figure 1, we performed three experiments.

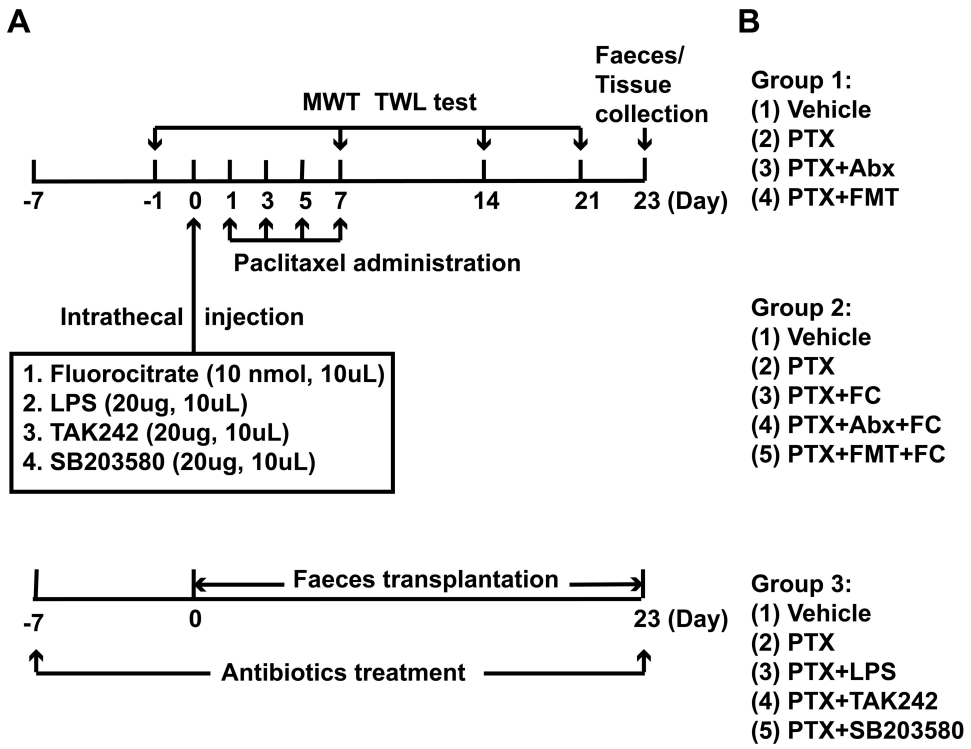

Figure 1 Experimental designs and animal groups. (**A**) Experimental design showing the administration of paclitaxel, transplanted fecal microbiota, and broad-spectrum antibiotics. (**B**) The first experiment investigated the effects of broad-spectrum antibiotics and transplanted fecal microbiota on mechanical allodynia and thermal hyperalgesia in PIPN rats. The second experiment investigated the effects of the astrocytic inhibitor fluorocitrate on mechanical allodynia and thermal hyperalgesia in PIPN rats. The third experiment investigated the effects of the TLR4 inhibitor (TAK242) and the p38 inhibitor (SB203580) on mechanical allodynia, thermal hyperalgesia, and astrocyte activity in PIPN rats.

Abbreviations: Abx, antibiotics; FC, fluorocitrate; FMT, fecal microbiota transplantation; LPS, lipopolysaccharide; MWT, mechanical withdrawal threshold measurements; PIPN, paclitaxel-induced peripheral neuropathy; PTX, paclitaxel; TWL, thermal withdrawal latency measurements.

First Experiment: Gut Microbiota Studies

To confirm whether gut microbiota dysbiosis is essential for promoting PIPN, 24 male rats were assigned to the Vehicle (intraperitoneal saline, n = 6) and PIPN (intraperitoneal paclitaxel, n = 18) groups randomly. Briefly, rats treated with paclitaxel (PTX) were randomly divided into three subgroups: the first subgroup received regular water (PTX, n = 6), the second subgroup received broad-spectrum antibiotics (PTX + Abx, n = 6), and the third group received the FMT from Vehicle rats (PTX + FMT, n = 6). MWTs and TWLs of rats were measured one day before paclitaxel administration and at Days 7, 14 and 21 following paclitaxel dosing. The colon and fecal samples were extracted at Day 23 and used for subsequent Western blotting, immunohistochemical staining, and 16S rDNA sequencing analysis.

Second Experiment: Investigation of Astrocyte Involvement

To confirm whether activated astrocytes are essential for the development of PIPN, we intrathecally administered the astrocytic inhibitor fluorocitrate in rats previously treated with paclitaxel. Specifically, we evaluated the behavioral changes and astrocyte activity in 15 male rats that were randomly assigned to the Vehicle (n = 3) and PIPN (n = 12) groups. Briefly, rats treated with paclitaxel were randomly divided into four subgroups: the first subgroup received intrathecal sterile saline (PTX group, n = 3), the second subgroup received fluorocitrate (PTX + FC group, n = 3), the third subgroup received fluorocitrate and broad-spectrum antibiotics (PTX + FC + Abx group, n = 3) and the fourth subgroup received fluorocitrate and FMT (PTX + FC + FMT group, n = 3). MWTs and TWLs were measured one day before paclitaxel dosing and at Days 7, 14 and 21 after paclitaxel dosing. The L3-L5 spinal region and spinal dorsal horn tissues were excised at Day 23 and used for subsequent immunohistochemical staining.

Third Experiment: Activation of the TLR4/p38 Pathway

To confirm whether activation of TLR4/p38 pathway is necessary to promote PIPN, we assigned 30 male rats to the Vehicle (n = 6) and PIPN (n = 24) groups randomly. Further, rats treated with paclitaxel were randomly divided into four subgroups (n = 6 each), ie, the PTX, PTX + LPS, PTX + TAK242, and PTX + SB203580 groups (hereafter, the Vehicle group is abbreviated as Vehicle, and the four subgroups are abbreviated as follows: PTX, PTX + LPS, PTX + TAK242, PTX + SB203580). The four subgroups were given intrathecal sterile saline, LPS, TLR4 inhibitor, and p38 inhibitor, respectively. Of note, the Vehicle group was administered intrathecal injections of sterile saline. MWTs and TWLs were measured one day before paclitaxel dosing and at Days 7, 14, and 21 after paclitaxel dosing. The L3-L5 spinal region and spinal dorsal horn tissues were excised at Day 23 and used for subsequent Western blotting and immunohistochemical staining.

Statistical Analysis

Investigators who were unaware of the study design analyzed all the data. Data were presented as mean ± standard deviation (SD). Statistical power was evaluated using SPSS software (version 25) while GraphPad Prism 8.0 software was employed for graph drawing. One-way or two-way analysis of variance (ANOVA) with a post-hoc Bonferroni test was used to determine the difference between groups. The Spearman correlation analysis was used to reveal the potential links between the microbiota and behavioral hypersensitivity. In all cases, significance was defined as p value < 0.05.

Results

Fecal Microbiota Transplantation (FMT) Alleviated Mechanical Allodynia and Thermal Hyperalgesia in Paclitaxel-Induced Peripheral Neuropathy (PIPN) Rats

Rats were treated with paclitaxel (intraperitoneal injection, 2 $mg \cdot kg^{-1}$) at Days 1, 3, 5 and 7. Compared with the Vehicle, PIPN rats showed peripheral neuropathy characterized by a marked reduction in MWTs and TWLs ($p < 0.001$, Figure 2A and B) in the hind paw, indicating that intraperitoneal injections of paclitaxel can induce mechanical allodynia and thermal hyperalgesia in rats. Seven days after acclimatization, fecal microbiota from Vehicle rats was transplanted in PIPN rats for 23 consecutive days, and the MWTs and TWLs were investigated at the baseline and at Days 7, 14 and 21. As shown in Figure 2A and B, FMT attenuated paclitaxel-induced mechanical allodynia and thermal hyperalgesia

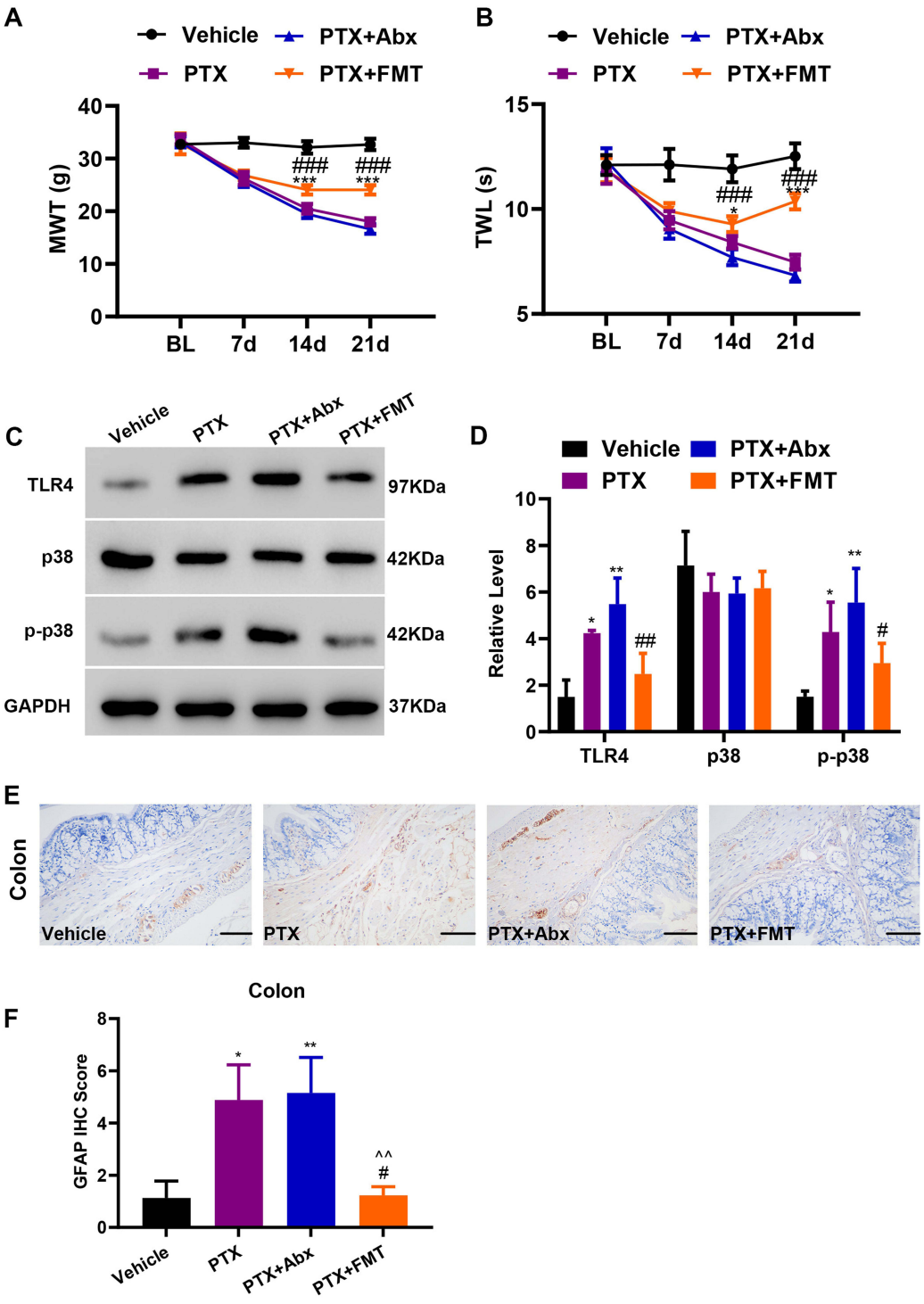

Figure 2 FMT alleviated mechanical allodynia and thermal hyperalgesia and suppressed the activation of the paclitaxel-induced pathways and astrocytes in PIPN rats. (**A**) The effects on mechanical allodynia in rats (Group × Time interaction: $F_{9,80} = 62.54$, $p < 0.0001$) (n = 6 rats per group). (**B**) The effects on thermal hyperalgesia in rats (Group × Time interaction: $F_{9,80} = 32.30$, $p < 0.0001$) (n = 6 rats per group). (**C** and **D**) Western blotting bands and analysis of TLR4, p-38, and p-p38 in the colon. $F_{3,12} = 19.57$ for TLR4, $F_{3,12} = 1.35$ for p38, $F_{3,12} = 10.56$ for p-p38. This experiment was repeated independently 4 times. (**E**) Photomicrographs representing glial fibrillary acidic protein immunoreactivity in each group. Scale bar = 200 μm. (**F**) Glial fibrillary acidic protein score. This experiment was independently repeated 3 times. Statistical comparison was performed by using two-way ANOVA followed by Bonferroni post-hoc test. Data are represented as mean ± standard deviation (SD). *$p < 0.05$, **$p < 0.01$ and ***$p < 0.001$ vs the Vehicle; $^{\#}p < 0.05$, $^{\#\#}p < 0.01$ and $^{\#\#\#}p < 0.001$ vs the PTX; $^{\wedge\wedge}p < 0.01$ compared with the PTX + Abx.

Abbreviations: Abx, antibiotics; FMT, fecal microbiota transplantation; GFAP, glial fibrillary acidic protein; PTX, paclitaxel.

significantly compared with the PTX ($p < 0.001$ for both), although not completely reverting them compared with the Vehicle ($p < 0.001$ for both). No differences were found between the PTX and PTX + Abx. In contrast, we found that FMT from the Vehicle rats significantly alleviated mechanical allodynia and thermal hyperalgesia in PIPN rats.

Fecal Microbiota Transplantation (FMT) Suppressed the Activation of the Paclitaxel-Induced Pathways and Astrocytes in Paclitaxel-Induced Peripheral Neuropathy (PIPN) Rats

To explore the molecular mechanisms of FMT functioning in PIPN rats, we characterized TLR4 and p38MAPK expression in colon tissues by Western blotting. The result indicated that paclitaxel administration significantly upregulated TLR4 and p-p38MAPK in the colon tissue ($p < 0.05$) (Figure 2C and D) in comparison with the Vehicle. TLR4 and p-p38MAPK were also highly expressed in the colon of the PIPN rats in the PTX + Abx. Compared with PIPN rats, Bonferroni post-hoc test indicated that FMT markedly inhibited TLR4 ($p < 0.01$) and p-p38MAPK ($p < 0.05$) expression, showing no difference with respect to the Vehicle. To verify whether gut microbiota participated in astrocyte activation in PIPN rats, we investigated GFAP in the colon by immunohistochemistry. Paclitaxel significantly upregulated GFAP expression ($p < 0.05$) (Figure 2E and F) in comparison with the Vehicle, similar to the result observed in the PTX + Abx ($p < 0.01$) in comparison with the Vehicle. FMT significantly reduced GFAP expression in the PTX + FMT in comparison with the PTX ($p < 0.05$) and the PTX + Abx ($p < 0.01$), suggesting that FMT from Vehicle rats suppressed the activation of astrocytes involved in paclitaxel-induced peripheral neuropathy.

Effects of Paclitaxel Administration on Gut Microbiota Diversity

Chemotherapy-induced neuroinflammation can disrupt the homeostasis of the colon in rodents.[44,45] Thus, we evaluated alterations in the gut microbiota composition among groups using the 16S rDNA gene sequencing. The Shannon index is a common way to measure the microbial diversity of a bacterial sample. Analysis of the α-diversity showed a significant decrease of diversity in the PTX in comparison with that in the Vehicle ($p < 0.05$) (Figure 3A); similarly, the diversity also decreased in the PTX + Abx in comparison with the Vehicle ($p < 0.01$) and the PTX ($p < 0.001$) (Figure 3A). While FMT reverted these effects similarly to the Vehicle. The Principal Coordinated Analysis (PCoA) is deployed to depict the relatedness of bacterial communities from different samples.[46] As shown in Figure 3B, principal component 1 (PC-1) and PC-2 explained 35.42% and 19.25% of the variance, respectively. Microbial differences were evident among the four groups, suggesting that the distribution of bacteria differed among the four groups. To further evaluate the variation of gut microbiota among groups, we selected the species with relatively high abundance in the colon (Figure 3C). The abundance of *Bacteroides* and *UCG-005* was elevated in the PTX compared to the Vehicle (Figure 3D and E). Conversely, the abundance of *Turicibacter, Clostridium_sensu_stricto_1* and *Corynebacterium* decreased in the PTX compared with the Vehicle (Figure 3F–H). Broad-spectrum antibiotics improved the quantity of *Romboutsia, Corynebacterium* and *Allobaculum* in PIPN rats, while decreased the abundance of *norank_f_Muribaculaceae* (Figure 3H–K). The relative abundance of *Lactobacillus, unclassified_f_Lachnospiraceae, Roseburia*, and *Eubacterium* was not different among groups (Figure 3L–O). Spearman correlation analysis clarified that the percentages of *Turicibacter, Clostridium_sensu_stricto_1* and *Corynebacterium* were negatively associated with MWTs (*R-value* = 1.000, $p < 0.001$) and TWLs (*R-value* = 0.986, $p < 0.001$) in the PTX. The abundance of *Bacteroides* was positively associated with MWTs (*R-value* = 1.000, $p < 0.001$) and TWLs (*R-value* = 0.986, $p < 0.001$) in the PTX. Similarly, the abundance of *UCG-005* was positively associated with MWTs (*R-value* = 0.986, $p < 0.001$) and TWLs (*R-value* = 0.956, $p = 0.003$) in the PTX.

Fluorocitrate Alleviated Mechanical Allodynia and Thermal Hyperalgesia in Paclitaxel-Induced Peripheral Neuropathy (PIPN) Rats

The astrocyte inhibitor fluorocitrate (FC, 10 nmol, 10 μL) was intrathecally injected one day before paclitaxel administration. We analyzed MWTs and TWLs at Days 0, 7, 14, and 21 in the following groups in the second experiment: Vehicle, PTX, PTX + FC, PTX + Abx + FC, and PTX + FMT + FC. At Day 21, MWTs ($p < 0.001$) and TWLs ($p < 0.05$) significantly increased in the PTX + FC in comparison with those in the PTX (Figure 4A and B). At Days 14 and 21, MWTs were increased ($p < 0.05$) in the PTX + FMT + FC in comparison with the PTX + FC, while MWTs were still lower in the PTX + FMT + FC than in the Vehicle ($p < 0.01$).

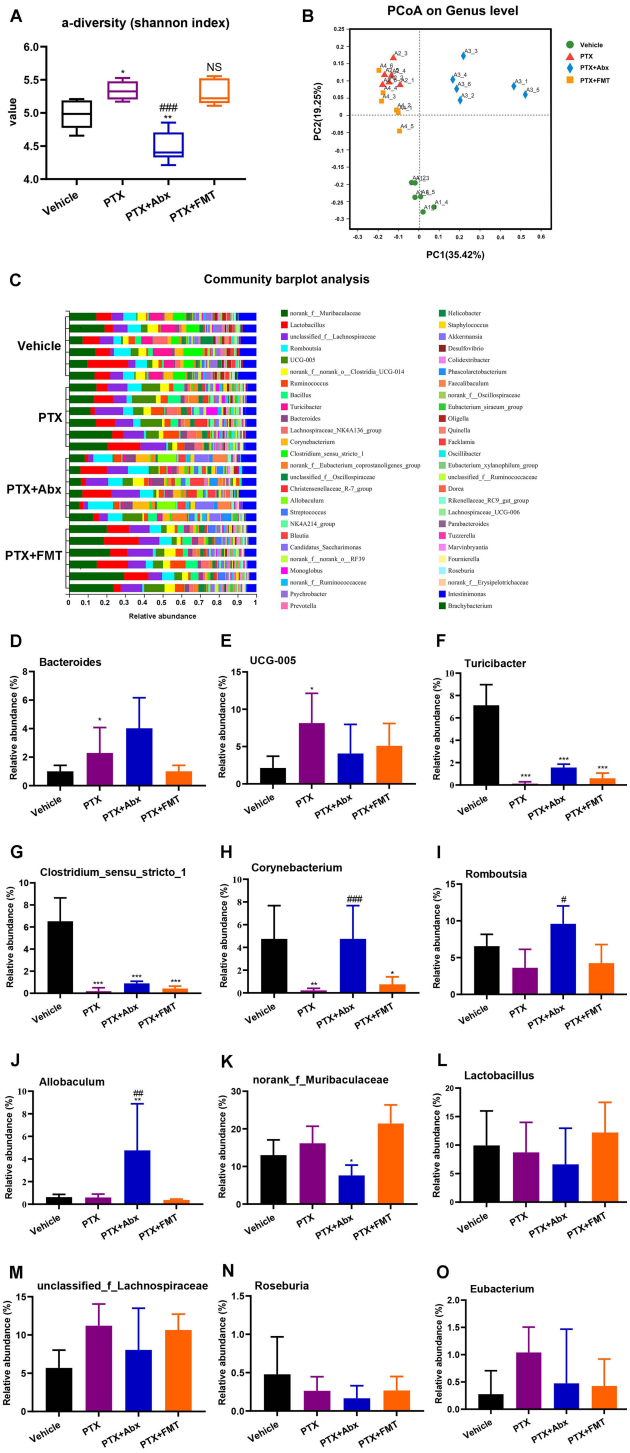

Figure 3 16S rDNA analysis of gut microbiota composition at the genus level. (**A**) The α-diversity Shannon index ($F_{3,20}$ = 24.19, p < 0.0001). (**B**) Dendrogram of β-diversity using the Principal Coordinated Analysis (PCoA) was used to analyze the gut microbiota in different groups. (**C**) Based on the quantitative data, the relative abundance of gut microbiota was displayed in a stacked bar plot. (**D**) Genus *Bacteroides* ($F_{3,20}$ = 6.037, p = 0.0042). (**E**) Genus *UCG-005* ($F_{3,20}$ = 3.554, p = 0.0328). (**F**) Genus *Turicibacter* ($F_{3,20}$ = 67.14, p < 0.0001). (**G**) Genus *Clostridium_sensu_stricto_1* ($F_{3,20}$ = 47.12, p < 0.0001). (**H**) Genus *Corynebacterium* ($F_{3,20}$ = 8.395, P = 0.0008). (**I**) Genus *Romboutsia* ($F_{3,20}$ = 8.290, p = 0.0009). (**J**) Genus *Allobaculum* ($F_{3,20}$ = 6.257, p = 0.0036). (**K**) Genus *norank_f_Muribaculaceae* ($F_{3,20}$ = 11.66, p = 0.0001). (**L**) Genus *Lactobacillus* ($F_{3,20}$ = 0.9852, p = 0.4197). (**M**) Genus *unclassified_f_Lachnospiraceae* ($F_{3,20}$ = 2.2, p = 0.12). (**N**) Genus *Roseburia* ($F_{3,20}$ = 1.247, P = 0.3191). (**O**) Genus *Eubacterium* ($F_{3,20}$ = 1.648, p = 0.2102). * p < 0.05, ** p < 0.01 and *** p < 0.001 compared with the Vehicle group. $^{\#}p$ < 0.05, $^{\#\#}p$ < 0.01 and $^{\#\#\#}p$ < 0.001 compared with the PTX group. NS, not significant compared with the vehicle group. Data are expressed as mean ± standard deviation (SD), with n = 6 rats per group.

Abbreviations: A1, Vehicle group; A2, PTX group; A3, PTX + Abx group; A4, PTX + FMT group; Abx, antibiotics; FMT, fecal microbiota transplantation; PTX, paclitaxel.

TWLs were decreased ($p < 0.05$) in the PTX + FC compared to the Vehicle. However, TWLs were not different between the PTX + FMT + FC and Vehicle ($p = 0.062$). Fluorocitrate has been shown to reduce mechanical allodynia and thermal hyperalgesia in rats with peripheral neuropathy-induced pain. When combined with FMT, the effect was enhanced but not completely reversed. In the lumbar spinal dorsal horn GFAP were upregulated in the PTX in comparison with the Vehicle, PTX + FC, PTX + Abx + FC and PTX + FMT + FC (Figure 4C and D). The GFAP expression level was not different among the Vehicle, PTX + FC and PTX + FMT + FC.

Inhibition of TLR4/p38MAPK Alleviated Mechanical Allodynia and Thermal Hyperalgesia and Suppressed Astrocyte Activation in Paclitaxel-Induced Peripheral Neuropathy (PIPN) Rats

To test whether the TLR4/p38MAPK pathway could modulate astrocyte activation in PIPN rats, we intrathecally injected single doses of LPS (a TLR4 agonist), TAK242 (selective TLR4 antagonist) and SB203580 (inhibitor of p38MAPK) the day before paclitaxel administration. Two-way ANOVA indicated that compared with the Vehicle, MWTs ($p < 0.0001$) (Figure 5A) and TWLs ($p < 0.0001$) (Figure 5B) were reduced after the administration of LPS. Injections of TAK242 and SB203580 increased MWTs and TWLs significantly ($p < 0.0001$) compared with those in the PTX throughout the experimental period. As displayed in Figure 5C and D, serum TNF-α and IL-1β were augmented ($p < 0.001$) in the PTX + LPS compared with the PTX but decreased ($p < 0.001$) in the PTX + TAK242 and PTX + SB203580 compared with the PTX. These results indicated that the TAK242 and SB203580 reduced TNF-α and IL-1β expression in PIPN rats. As displayed in Figure 5E and F, injection of LPS significantly increased the p-p38MAPK expression in the colon compared with the PTX ($p < 0.01$). Injections of TAK242 and SB203580 reduced the expression of p-p38MAPK, with no difference among the Vehicle, PTX + TAK242 and PTX + SB203580. The results were consistent with those of the first experiment, showing that FMT suppressed the activation of TLR4/p38 pathways in the colon. As shown in Figure 5G and H, injection of LPS significantly increased the GFAP level in the spinal dorsal horn tissues compared to the Vehicle ($p < 0.001$). The PTX + TAK242 and PTX + SB203580 significantly decreased the GFAP level compared to the PTX ($p < 0.001$). These results indicated that the TLR4/p38MAPK pathway could modulate astrocyte activation in the spinal dorsal horn in PIPN rats.

Discussion

We explored the therapeutic role of gut microbiota in rat PIPN, showing that FMT from normal rats decreased MWTs and TWLs in the hind paws, without abolishing them altogether. These findings have been recently replicated in mice with neuropathic pain caused by various forms of injury or diseases.[47] Moreover, FMT reduced astrocyte activity and TLR4/p38MAPK signals in the colon and the spinal dorsal horn tissues of PIPN rats. These findings revealed the underlying mechanisms of FMT in promoting antinociception against PIPN.

Consistent with previous research,[35,48] we established a PIPN model of rats with a final cumulative dose of intraperitoneal paclitaxel around 8 $mg \cdot kg^{-1}$. In our first experiment, we administered broad-spectrum antibiotics or transplanted fecal microbiota to assess the effects of gut microbiota on behavioral hypersensitivity in PIPN rats. In contrast to previous studies conducted in oxaliplatin-induced mice[38,47] and B6-B6mb mice receiving paclitaxel,[31] we showed that depleting gut microbiota with broad-spectrum antibiotics aggravated mechanical allodynia and thermal hyperalgesia. Inter-individual variation in the gut microbiota composition might also lead to individualized host responses.[49] Specific microbial species associated with microbiota initial state may determine a personalized response to treatments.[50] Although the reason for the aforementioned discrepancy is unclear, the initial state of the microbiota in animals receiving different chemotherapeutic drugs may have played a role in explaining it.

The gut microbiota regulates peripheral and central sensitization. Altered gut microbiota profiles of rats (eg, broad-spectrum antibiotics treatment or FMT) provided an opportunity to assess the association between behavioral and inflammatory responses in PIPN rats. The diversity results from the indices showed that *Turicibacter, Clostridium sensu stricto 1, Corynebacterium, Bacteroides*, and *UCG-005* might exert certain effects on the development of PIPN. Two recent studies reported that the relative abundance of *Bacteroides*, and *UCG-005* may promote painful manifestations in rodents.[47,51] In our study, the abundance of *Lactobacillus, unclassified f Lachnospiraceae, Roseburia*, and

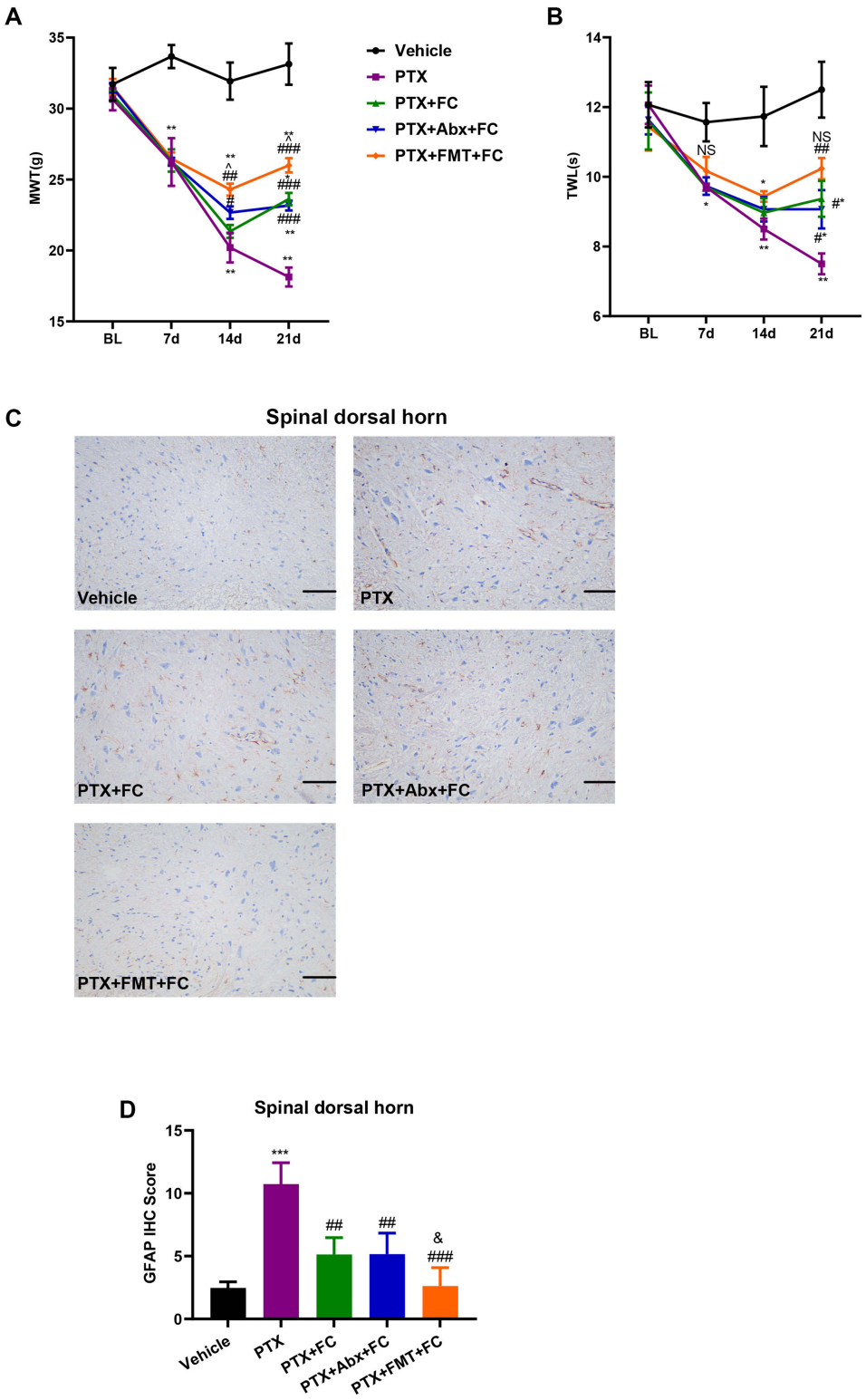

Figure 4 Fluorocitrate alleviated mechanical allodynia and thermal hyperalgesia in PIPN rats. (**A**) The effect on mechanical allodynia in rats (Group × Time interaction: $F_{12,40}$ = 26.05, $p < 0.0001$) (n = 3 rats per group). (**B**) The effect on thermal hyperalgesia in rats (Group × Time interaction: $F_{12,40}$ = 7.296, $p < 0.0001$) (n = 3 rats per group). (**C**) Immunohistochemical micrograph representing glial fibrillary acidic protein immunoreactivity in the spinal dorsal horns for each group. Scale bar = 200 μm. (**D**) Glial fibrillary acidic protein scores in the spinal dorsal horns. $F_{4,10}$ = 16.99 for (**D**). This experiment was independently repeated 3 times. $^{*}p < 0.05$, $^{**}p < 0.01$ and $^{***}p < 0.001$ compared with the Vehicle. $^{\#}p < 0.05$, $^{\#\#}p < 0.01$ and $^{\#\#\#}p < 0.001$ compared with the PTX. $^{\wedge}p < 0.05$ compared with the PTX + FC. NS, not significant compared with the Vehicle group. &, not significant compared with the PTX + FC.

Abbreviations: Abx, antibiotics; BL, baseline; d, day; FC, fluorocitrate; GFAP, glial fibrillary acidic protein; PTX, paclitaxel.

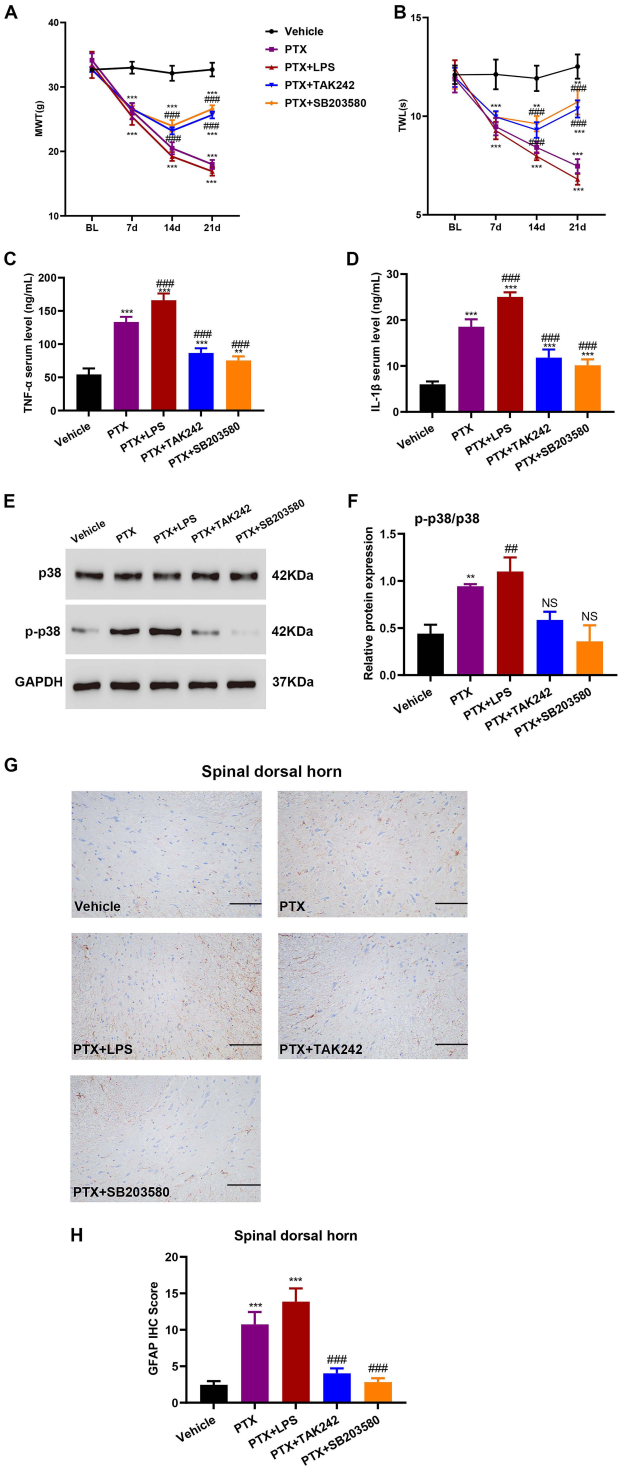

Figure 5 Inhibition of TLR4/p38MAPK alleviated mechanical allodynia and thermal hyperalgesia and suppressed astrocyte activation in PIPN rats. (**A**) The effect on mechanical allodynia in rats (Group × Time interaction: $F_{12,100} = 71$, $p < 0.0001$) (n = 6 rats per group). (**B**) The effect on thermal hyperalgesia in rats (Group × Time interaction: $F_{12,100} = 30.05$, $p < 0.0001$) (n = 6 rats per group). (**C** and **D**) Serum levels of TNF-α and IL-1β measured by enzyme-linked immunosorbent assay kits. (**E** and **F**) Western blotting bands and analysis of p-38 and p-p38 expression in the colon. $F_{4,10} = 0.6633$ for p38 and $F_{4,10} = 23.21$ for p-p38. This experiment was independently repeated 3 times. (**G**) Immunohistochemical micrograph representing glial fibrillary acidic protein immunoreactivity in the spinal dorsal horns for each group. Scale bar = 200 μm. (**H**) Glial fibrillary acidic protein scores in the spinal dorsal horns. $F_{4,10} = 55.76$ for (**H**). This experiment was independently repeated 3 times. $^{**}p < 0.01$ and $^{***}p < 0.001$ compared with the Vehicle group. $^{\#\#}p < 0.01$ and $^{\#\#\#}p < 0.001$ compared with the PTX group. NS, not significant compared with the Vehicle group.

Abbreviations: BL, baseline; d, day; GFAP, glial fibrillary acidic protein; LPS, lipopolysaccharide; PTX, paclitaxel.

https://doi.org/10.2147/JPR.S415642 DovePress

Eubacterium was comparable among groups. The future identification of microbial species contributing to mechanical allodynia and thermal hyperalgesia in PIPN might provide the rationale for novel therapeutic targets.

Through microbial metabolites, the gut microbiota interacts with ganglia in the spinal cord and dorsal root tissues.[52,53] Several mediators (eg, IL-1β, TNF-α, short-chain fatty acids, and bile acids) reportedly have a critical role in the development of neuropathic pain by regulating the peripheral and central sensitization.[54,55] Activation of astrocytes and microglial cells promotes the release of cytokines and chemokines, altering glutamatergic and GABAergic neurotransmissions, ultimately leading to pain hypersensitivity. Activation of astrocytes has been previously involved in the development of PIPN.[16,17] We found upregulated GFAP levels in the colon and lumbar spinal dorsal horn tissues of PIPN rats. A single injection of fluorocitrate (an inhibitor for astrocytes) reduced mechanical allodynia and thermal hyperalgesia in PIPN rats. Of note, FMT showed synergistic effects on mechanical allodynia and thermal hyperalgesia.

LPS activates TLR4 signaling from the surface of astrocytes, which is involved in neuron-immune interactions and pain processing.[56] TLR4 activation involves signaling in two different ways. One triggers the MyD88-dependent cascade, causing the early activation of NF-κB, followed by the synthesis and release of several cytokines and chemokines. Another is induced by TIR-domain-containing adapter-inducing interferon-β (TRIF), causing delayed NF-κB and interferon-β production.[57,58] In addition to typical signaling pathways, the MAPK signaling cascade is also involved in activating TLR4.[12] TLR4 recruits p38 signaling and SB203580 (a p38 inhibitor) reduces the LPS-induced expression of IL-1 and TNF-α.[56,59] In accordance with previous research, we found that TLR4 and its downstream p38MAPK may potentially contribute to the generation of PIPN. Elimination of gut microbiota by broad-spectrum antibiotics significantly enhanced the activity of the TLR4/p38 signaling pathway in response to LPS, while FMT from Vehicle rats reduced the TLR4/p38 signaling activity induced by intrathecal injections of TAK242 and SB203580. In addition, inhibition of the TLR4/p38 pathway decreased GFAP expression in the spinal dorsal horn tissues, suggesting that FMT alleviated the behavioral hypersensitivity in PIPN rats by blocking the TLR4/p38 pathway.[11,60] Therefore, we conclude that gut microbiota might play a significant role in suppressing the activation of the TLR4/p38 pathway and astrocytes in PIPN rats.

Our study has some limitations. First, we only collected feces from rats for 16S rDNA analysis in the first experiment. However, we did not collect feces from rats in the second and third experiments, despite confirming that changes in gut microbiota can alleviate mechanical allodynia and thermal hyperalgesia in PIPN rats. It is important to note that FMT approach does not always lead to sustainable microbiome changes as one would expect, and further research is necessary to identify the key gut microbiota species involved. Second, we only used male rats and did not investigate the potential role of sex differences in gut microbiota composition in PIPN rats. Therefore, further research should be conducted to explore the effects of FMT on sex differences in mechanical allodynia and thermal hyperalgesia in PIPN rats.

Conclusion

In summary, FMT alleviated mechanical allodynia and thermal hyperalgesia in PIPN rats. Reduced pain behaviors may be caused by the compromised TLR4/p38 pathway or astrocyte activity in the colon and spinal dorsal horn tissues. We suggest that FMT may be a potential therapy for PIPN.

Acknowledgments

This study is funded by the Zhejiang Provincial Medical and Health Science and Technology Project of China (Grant Numbers 2020KY231 and 2022KY943). The authors acknowledge TopEdit LLC for the linguistic editing and proofreading during the preparation of this manuscript.

Disclosure

All authors declare that they have no conflicts of interest in this work.

References

1. Wallington M, Saxon EB, Bomb M, et al. 30-day mortality after systemic anticancer treatment for breast and lung cancer in England: a population-based, observational study. *Lancet Oncol*. 2016;17(9):1203–1216. doi:10.1016/s1470-2045(16)30383-7

2. Shetti D, Zhang B, Fan C, Mo C, Lee BH, Wei K. Low dose of paclitaxel combined with XAV939 attenuates metastasis, angiogenesis and growth in breast cancer by suppressing wnt signaling. *Cells*. 2019;8(8):1. doi:10.3390/cells8080892
3. Ansari MA, Thiruvengadam M, Farooqui Z, et al. Nanotechnology, in silico and endocrine-based strategy for delivering paclitaxel and miRNA: prospects for the therapeutic management of breast cancer. *Semin Cancer Biol*. 2021;69:109–128. doi:10.1016/j.semcancer.2019.12.022
4. Walker JL, Brady MF, Wenzel L, et al. Randomized trial of intravenous versus intraperitoneal chemotherapy plus bevacizumab in advanced ovarian carcinoma: an NRG oncology/gynecologic oncology group study. *J Clin Oncol*. 2019;37(16):1380–1390. doi:10.1200/jco.18.01568
5. Powell MA, Filiaci VL, Hensley ML, et al. Randomized phase III trial of paclitaxel and carboplatin versus paclitaxel and ifosfamide in patients with carcinosarcoma of the uterus or ovary: an NRG oncology trial. *J Clin Oncol*. 2022;40(9):968–977. doi:10.1200/jco.21.02050
6. Yoneshima Y, Morita S, Ando M, et al. Phase 3 trial comparing nanoparticle albumin-bound paclitaxel with docetaxel for previously treated advanced NSCLC. *J Thorac Oncol*. 2021;16(9):1523–1532. doi:10.1016/j.jtho.2021.03.027
7. Klein I, Lehmann HC. Pathomechanisms of paclitaxel-induced peripheral neuropathy. *Toxics*. 2021;9(10). doi:10.3390/toxics9100229
8. Sisignano M, Baron R, Scholich K, Geisslinger G. Mechanism-based treatment for chemotherapy-induced peripheral neuropathic pain. *Nat Rev Neurol*. 2014;10(12):694–707. doi:10.1038/nrneurol.2014.211
9. da Costa R, Passos GF, Quintão NLM, et al. Taxane-induced neurotoxicity: pathophysiology and therapeutic perspectives. *Br J Pharmacol*. 2020;177(14):3127–3146. doi:10.1111/bph.15086
10. Oladiran O, Shi XQ, Yang M, Fournier S, Zhang J. Inhibition of TLR4 signaling protects mice from sensory and motor dysfunction in an animal model of autoimmune peripheral neuropathy. *J Neuroinflammation*. 2021;18(1):77. doi:10.1186/s12974-021-02126-x
11. Li Y, Yin C, Li X, et al. Electroacupuncture alleviates paclitaxel-induced peripheral neuropathic pain in rats via suppressing TLR4 signaling and TRPV1 upregulation in sensory neurons. *Int J Mol Sci*. 2019;20(23). doi:10.3390/ijms20235917
12. Li Y, Zhang H, Kosturakis AK, et al. MAPK signaling downstream to TLR4 contributes to paclitaxel-induced peripheral neuropathy. *Brain Behav Immun*. 2015;49:255–266. doi:10.1016/j.bbi.2015.06.003
13. Li Y, Zhang H, Zhang H, Kosturakis AK, Jawad AB, Dougherty PM. Toll-like receptor 4 signaling contributes to Paclitaxel-induced peripheral neuropathy. *J Pain*. 2014;15(7):712–725. doi:10.1016/j.jpain.2014.04.001
14. Ba X, Wang J, Zhou S, et al. Cinobufacini protects against paclitaxel-induced peripheral neuropathic pain and suppresses TRPV1 up-regulation and spinal astrocyte activation in rats. *Biomed Pharmacother*. 2018;108:76–84. doi:10.1016/j.biopha.2018.09.018
15. Hu Q, Zheng X, Li X, et al. Electroacupuncture alleviates mechanical allodynia in a rat model of complex regional pain syndrome type-I via suppressing spinal CXCL12/CXCR4 signaling. *J Pain*. 2020;21(9–10):1060–1074. doi:10.1016/j.jpain.2020.01.007
16. Liu X, Tonello R, Ling Y, Gao YJ, Berta T. Paclitaxel-activated astrocytes produce mechanical allodynia in mice by releasing tumor necrosis factor-α and stromal-derived cell factor 1. *J Neuroinflammation*. 2019;16(1):209. doi:10.1186/s12974-019-1619-9
17. Li DY, Gao SJ, Sun J, et al. Notch signaling activation contributes to paclitaxel-induced neuropathic pain via activation of A1 astrocytes. *Eur J Pharmacol*. 2022;928:175130. doi:10.1016/j.ejphar.2022.175130
18. Dinan TG, Cryan JF. Microbes, immunity, and behavior: psychoneuroimmunology meets the microbiome. *Neuropsychopharmacology*. 2017;42 (1):178–192. doi:10.1038/npp.2016.103
19. Plaza-Díaz J, Álvarez-Mercado AI, Ruiz-Marín CM, et al. Association of breast and gut microbiota dysbiosis and the risk of breast cancer: a case-control clinical study. *BMC Cancer*. 2019;19(1):495. doi:10.1186/s12885-019-5660-y
20. von Schwartzenberg RJ, Bisanz JE, Lyalina S, et al. Caloric restriction disrupts the microbiota and colonization resistance. *Nature*. 2021;595 (7866):272–277. doi:10.1038/s41586-021-03663-4
21. Wu J, Wei Z, Cheng P, et al. Rhein modulates host purine metabolism in intestine through gut microbiota and ameliorates experimental colitis. *Theranostics*. 2020;10(23):10665–10679. doi:10.7150/thno.43528
22. Asnicar F, Berry SE, Valdes AM, et al. Microbiome connections with host metabolism and habitual diet from 1098 deeply phenotyped individuals. *Nat Med*. 2021;27(2):321–332. doi:10.1038/s41591-020-01183-8
23. Hegelmaier T, Lebbing M, Duscha A, et al. Interventional influence of the intestinal microbiome through dietary intervention and bowel cleansing might improve motor symptoms in Parkinson's disease. *Cells*. 2020;9(2). doi:10.3390/cells9020376
24. Vascellari S, Melis M, Cossu G, et al. Genetic variants of TAS2R38 bitter taste receptor associate with distinct gut microbiota traits in Parkinson's disease: a pilot study. *Int J Biol Macromol*. 2020;165(Pt A):665–674. doi:10.1016/j.ijbiomac.2020.09.056
25. Cox SR, Lindsay JO, Fromentin S, et al. Effects of low FODMAP diet on symptoms, fecal microbiome, and markers of inflammation in patients with quiescent inflammatory bowel disease in a randomized trial. *Gastroenterology*. 2020;158(1):176–188.e7. doi:10.1053/j.gastro.2019.09.024
26. El-Salhy M, Hatlebakk JG, Gilja OH, Bråthen Kristoffersen A, Hausken T. Efficacy of faecal microbiota transplantation for patients with irritable bowel syndrome in a randomised, double-blind, placebo-controlled study. *Gut*. 2020;69(5):859–867. doi:10.1136/gutjnl-2019-319630
27. Zhuang Z, Yang R, Wang W, Qi L, Huang T. Associations between gut microbiota and Alzheimer's disease, major depressive disorder, and schizophrenia. *J Neuroinflammation*. 2020;17(1):288. doi:10.1186/s12974-020-01961-8
28. Li S, Song J, Ke P, et al. Author Correction: the gut microbiome is associated with brain structure and function in schizophrenia. *Sci Rep*. 2021;11 (1):17643. doi:10.1038/s41598-021-96985-2
29. Chen P, Wang C, Ren YN, Ye ZJ, Jiang C, Wu ZB. Alterations in the gut microbiota and metabolite profiles in the context of neuropathic pain. *Mol Brain*. 2021;14(1):50. doi:10.1186/s13041-021-00765-y
30. Ding W, You Z, Chen Q, et al. Gut microbiota influences neuropathic pain through modulating proinflammatory and anti-inflammatory T cells. *Anesth Analg*. 2021;132(4):1146–1155. doi:10.1213/ane.0000000000005155
31. Ramakrishna C, Corleto J, Ruegger PM, et al. Dominant role of the gut microbiota in chemotherapy induced neuropathic pain. *Sci Rep*. 2019;9 (1):20324. doi:10.1038/s41598-019-56832-x
32. Cuozzo M, Castelli V, Avagliano C, et al. Effects of chronic oral probiotic treatment in paclitaxel-induced neuropathic pain. *Biomedicines*. 2021;9 (4). doi:10.3390/biomedicines9040346
33. Sun MF, Zhu YL, Zhou ZL, et al. Neuroprotective effects of fecal microbiota transplantation on MPTP-induced Parkinson's disease mice: gut microbiota, glial reaction and TLR4/TNF-α signaling pathway. *Brain Behav Immun*. 2018;70:48–60. doi:10.1016/j.bbi.2018.02.005
34. Zhao Z, Li F, Ning J, et al. Novel compound FLZ alleviates rotenone-induced PD mouse model by suppressing TLR4/MyD88/NF-κB pathway through microbiota-gut-brain axis. *Acta Pharm Sin B*. 2021;11(9):2859–2879. doi:10.1016/j.apsb.2021.03.020

35. Zhang H, Li Y, de Carvalho-Barbosa M, et al. Dorsal root ganglion infiltration by macrophages contributes to paclitaxel chemotherapy-induced peripheral neuropathy. *J Pain*. 2016;17(7):775–786. doi:10.1016/j.jpain.2016.02.011
36. Boyette-Davis J, Xin W, Zhang H, Dougherty PM. Intraepidermal nerve fiber loss corresponds to the development of taxol-induced hyperalgesia and can be prevented by treatment with minocycline. *Pain*. 2011;152(2):308–313. doi:10.1016/j.pain.2010.10.030
37. Ge X, Zhao W, Ding C, et al. Potential role of fecal microbiota from patients with slow transit constipation in the regulation of gastrointestinal motility. *Sci Rep*. 2017;7(1):441. doi:10.1038/s41598-017-00612-y
38. Shen S, Lim G, You Z, et al. Gut microbiota is critical for the induction of chemotherapy-induced pain. *Nat Neurosci*. 2017;20(9):1213–1216. doi:10.1038/nn.4606
39. Liang T, Chen XF, Yang Y, et al. Secondary damage and neuroinflammation in the spinal dorsal horn mediate post-thalamic hemorrhagic stroke pain hypersensitivity: SDF1-CXCR4 signaling mediation. *Front Mol Neurosci*. 2022;15:911476. doi:10.3389/fnmol.2022.911476
40. Saito O, Svensson CI, Buczynski MW, et al. Spinal glial TLR4-mediated nociception and production of prostaglandin E(2) and TNF. *Br J Pharmacol*. 2010;160(7):1754–1764. doi:10.1111/j.1476-5381.2010.00811.x
41. Qian J, Zhu Y, Bai L, et al. Chronic morphine-mediated upregulation of high mobility group box 1 in the spinal cord contributes to analgesic tolerance and hyperalgesia in rats. *Neurotherapeutics*. 2020;17(2):722–742. doi:10.1007/s13311-019-00800-w
42. Li T, Liu T, Chen X, et al. Microglia induce the transformation of A1/A2 reactive astrocytes via the CXCR7/PI3K/Akt pathway in chronic post-surgical pain. *J Neuroinflammation*. 2020;17(1):211. doi:10.1186/s12974-020-01891-5
43. Lin J, Ren J, Zhu B, et al. Dimethyl itaconate attenuates CFA-induced inflammatory pain via the NLRP3/ IL-1β signaling pathway. *Front Pharmacol*. 2022;13:938979. doi:10.3389/fphar.2022.938979
44. Loman BR, Jordan KR, Haynes B, Bailey MT, Pyter LM. Chemotherapy-induced neuroinflammation is associated with disrupted colonic and bacterial homeostasis in female mice. *Sci Rep*. 2019;9(1):16490. doi:10.1038/s41598-019-52893-0
45. Rashidi A, Kaiser T, Shields-Cutler R, et al. Dysbiosis patterns during re-induction/salvage versus induction chemotherapy for acute leukemia. *Sci Rep*. 2019;9(1):6083. doi:10.1038/s41598-019-42652-6
46. Yang C, Fang X, Zhan G, et al. Key role of gut microbiota in anhedonia-like phenotype in rodents with neuropathic pain. *Transl Psychiatry*. 2019;9(1):57. doi:10.1038/s41398-019-0379-8
47. Ma P, Mo R, Liao H, et al. Gut microbiota depletion by antibiotics ameliorates somatic neuropathic pain induced by nerve injury, chemotherapy, and diabetes in mice. *J Neuroinflammation*. 2022;19(1):169. doi:10.1186/s12974-022-02523-w
48. Zhao YX, Yao MJ, Liu Q, Xin JJ, Gao JH, Yu XC. Electroacupuncture treatment attenuates paclitaxel-induced neuropathic pain in rats via inhibiting spinal glia and the TLR4/NF-κB pathway. *J Pain Res*. 2020;13:239–250. doi:10.2147/jpr.S241101
49. Lavelle A, Hoffmann TW, Pham HP, Langella P, Guédon E, Sokol H. Baseline microbiota composition modulates antibiotic-mediated effects on the gut microbiota and host. *Microbiome*. 2019;7(1):111. doi:10.1186/s40168-019-0725-3
50. Rashidi A, Ebadi M, Rehman TU, et al. Gut microbiota response to antibiotics is personalized and depends on baseline microbiota. *Microbiome*. 2021;9(1):211. doi:10.1186/s40168-021-01170-2
51. Shen CL, Wang R, Ji G, et al. Dietary supplementation of gingerols- and shogaols-enriched ginger root extract attenuate pain-associated behaviors while modulating gut microbiota and metabolites in rats with spinal nerve ligation. *J Nutr Biochem*. 2022;100:108904. doi:10.1016/j.jnutbio.2021.108904
52. Tang AT, Choi JP, Kotzin JJ, et al. Endothelial TLR4 and the microbiome drive cerebral cavernous malformations. *Nature*. 2017;545(7654):305–310. doi:10.1038/nature22075
53. Duan L, Zhang XD, Miao WY, et al. PDGFRβ cells rapidly relay inflammatory signal from the circulatory system to neurons via chemokine CCL2. *Neuron*. 2018;100(1):183–200.e8. doi:10.1016/j.neuron.2018.08.030
54. Matsuda M, Huh Y, Ji RR. Roles of inflammation, neurogenic inflammation, and neuroinflammation in pain. *J Anesth*. 2019;33(1):131–139. doi:10.1007/s00540-018-2579-4
55. Chen G, Zhang YQ, Qadri YJ, Serhan CN, Ji RR. Microglia in pain: detrimental and protective roles in pathogenesis and resolution of pain. *Neuron*. 2018;100(6):1292–1311. doi:10.1016/j.neuron.2018.11.009
56. Birla H, Xia J, Gao X, et al. Toll-like receptor 4 activation enhances Orai1-mediated calcium signal promoting cytokine production in spinal astrocytes. *Cell Calcium*. 2022;105:102619. doi:10.1016/j.ceca.2022.102619
57. O'Neill LA, Bowie AG. The family of five: TIR-domain-containing adaptors in Toll-like receptor signalling. *Nat Rev Immunol*. 2007;7(5):353–364. doi:10.1038/nri2079
58. Pålsson-McDermott EM, O'Neill LA. Signal transduction by the lipopolysaccharide receptor, Toll-like receptor-4. *Immunology*. 2004;113(2):153–162. doi:10.1111/j.1365-2567.2004.01976.x
59. Guan HY, Xia HX, Chen XY, Wang L, Tang ZJ, Zhang W. Toll-like receptor 4 inhibits estradiol secretion via NF-κB signaling in human granulosa cells. *Front Endocrinol*. 2021;12:629554. doi:10.3389/fendo.2021.629554
60. Chen Y, Lu R, Wang Y, Gan P. Shaoyao gancao decoction ameliorates paclitaxel-induced peripheral neuropathy via suppressing TRPV1 and TLR4 signaling expression in rats. *Drug Des Devel Ther*. 2022;16:2067–2081. doi:10.2147/dddt.S357638